Quantum Transport Mode in Graphene Nanoribbon Based Transistor

Article *in* Journal of Nanoelectronics and Optoelectronics · September 2017

DOI: 10.1166/jno.2017.2097

5 authors, including:

Mohammad Taghi Ahmadi
Universiti Teknologi Malaysia
219 PUBLICATIONS **1,015** CITATIONS
SEE PROFILE

Hadi Goudarzi
Urmia University
60 PUBLICATIONS **145** CITATIONS
SEE PROFILE

Shahram Moradi
Middle East Technical University
8 PUBLICATIONS **47** CITATIONS
SEE PROFILE

Journal of
Nanoelectronics and Optoelectronics
Vol. 12, pp. 1–5, 2017
www.aspbs.com/jno

ARTICLE

Quantum Transport Mode in Graphene Nanoribbon Based Transistor

Sayed Norollah Hedayat[1,*], Mohammad Taghi Ahmadi[1], Hassan Sedghi[1], Hadi Goudarzi[1], and Shahram Moradi[2]

Graphene has incredible carrier transport property with high application opportunity at single molecule level, which composes it as promising materials on nano electronic application. In order to develop the new device such as graphene nanoribbon transistor, Carbon Nanotube Field Effect Transistor (CNTFET) and nanowire based devices, it is essential to investigate the quantum limit in low dimensional systems. In this paper transmission coefficient of the schottky structure in the graphene based transistor is modeled additionally its quantum properties due to the structural parameters are analyzed. Also one dimensional quantum current in the presence of the wave vector approximation for monolayer graphene nanoribbon (MGNR) is presented.

Keywords: Quantum Current, Degenerate and Nondegenerate Approximation, Graphene Nanoribbons, Transmission Coefficient, Monolayer Graphene.

1. INTRODUCTION

Recently carbon based materials such as graphene nanoribbon has been studied extensively.[1–4] Graphene nanoribbon (GNR) as a monolayer graphite with nanometer width indicates excellent electrical and optical[5,6] properties. Thus in all related fields including transistor fabrication[7] interconnecting circuitry,[8] electromechanical switches[9] infrared emitters and bio-sensors have been employed widely.[10,11] Furthermore, the electronic structure of graphene and its low scattering rate lead in desirable electronic transmission, compatibility of doping and utilization on electrostatic area. Particular nature of graphene's charge carriers made it important component.[12,13] Even long mean free path and also electron–electron interactions with high level of electron scattering exist in graphene.[14,15] By considering all these unique properties of carbon nanostructures specially GNRs with distinguished properties it is completely accepted as a promising component in future electronic technology.[16,17] As shown in Figure 1 the schematic of GNR transistor with two schottky contact is considered this structure can be made by top-down fabrication method.

In an atomic level the approach of top-down is so efficient to particular control over the width and edge termination of the nanoribbon.[18,19] And the fabrication of mentioned structure can be achieved by oxygen plasma etching[23–25] the proposed structure is employed as a transistor platform in the analytical modeling.

2. MODEL

By using Tight-binding method GNRs in *ab-initio* the nonzero direct band gap of hydrogen termination of either armchair or zigzag shaped edges have been estimated. The proportionality of two parameters in GNRs width and E_g (band gap energy) has been reported. Numerous computation for various structures by moving one layer over the other in which the atoms are locating at the center of hexagons in the upper layer and in the direction of the infinite edge has been done.[20–22] The engineered graphene with armchair structure with 0.22 eV has been reported. By increasing the thickness of the sample E_g starts to decrease and finally become zero. This observation provides a promising proportionality of graphene band gap engineering. Band energy calculation as a key fundamental parameter based on the tight-binding method has been reported as:

$$E(\vec{k}) = \pm t\sqrt{1+4\cos\left(\frac{k_x 3a_{c-c}}{2}\right)\cos\left(\frac{k_y\sqrt{3}a_{c-c}}{2}\right)+4\cos^2\left(\frac{k_y\sqrt{3}a_{c-c}}{2}\right)} \quad (1)$$

[1]Department of Physics, Faculty of Science, Urmia University, 75175, Urmia, Iran
[2]Department of Electrical Engineering, Middle East Technical University, Ankara, Turkey
*Author to whom correspondence should be addressed.
Email: sn.hedayat@yahoo.com
Received: 8 December 2016
Accepted: 19 February 2017

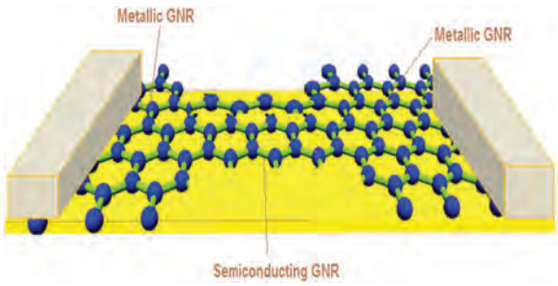

Fig. 1. Schematic of two Schottky contacts of metallic grapheme with semiconducting in the channel region.

Where k_x, k_y are the wave vector next to the extent of the nanoribbon and a_{c-c} is the carbon–carbon band length, on the other hand the presented model can be modified as:[13]

$$E(\vec{k}) = \pm\frac{3a_{c-c}t}{2}\sqrt{k_x^2+\beta^2} \tag{2}$$

Where $\beta = (2\pi/(a_{c-c}\sqrt{3}))(p_i/(N+1)-2/3)$ the quantized wave vector and N is the number of dimmer appearance which, determine the thickness of the ribbon and p_i is the sub band directory. The modified one dimensional dispersion relation for the further development is considered and the transmission amplitudes for a single square barrier centered at the origin with height V_0 and width bas shown in the Figure 2 is analytically modeled. It has been demonstrated that one semiconducting GNR can be sandwiched between two metallic GNR, consequently the difference between metallic and semiconducting Fermi levels creates barrier in each side therefore a square quantum barrier can be assumed as shown in Figure 2.

An electron as a particle has been described by a wave function which is continues function. When an electron bumps with several boundaries its wave function must have

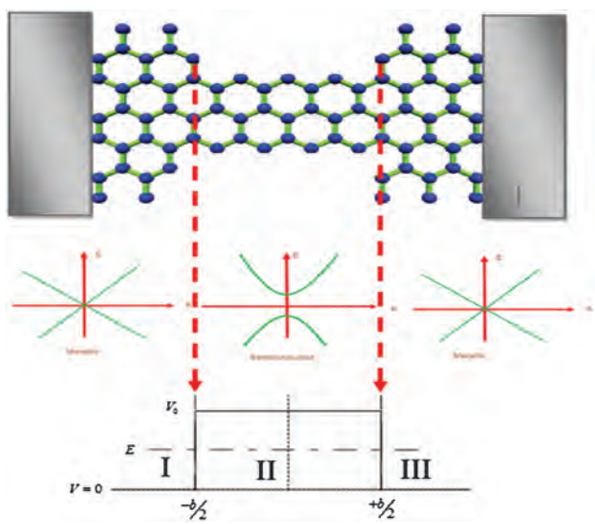

Fig. 2. Channel region barrier in GNR based contact with semiconducting GNR sandwiched between two metallic GNR.

a different form in each region but these functions must match in the boundaries. The transistor operation can be modeled in the form of three different regions as shown in Figure 2 which leads to the Schrödinger equation result for potential of each region as:

$$V(x) = \begin{cases} 0, & x < \dfrac{-b}{2} \\ V_0, & \dfrac{-b}{2} < x < \dfrac{b}{2} \rightarrow \psi(x) \\ 0, & x > \dfrac{b}{2} \end{cases}$$

$$= \begin{cases} A_n e^{ikx} + B_n e^{-ikx}, & x < \dfrac{-b}{2} \\ Ce^{-Kx} + De^{Kx}, & \dfrac{-b}{2} < x < \dfrac{b}{2} \\ A_{n+1}e^{ikx} + B_{n+1}e^{-ikx}, & x > \dfrac{b}{2} \end{cases} \tag{3}$$

Where wave number in first and third regions is $k = \sqrt{2mE/\hbar^2}$, and the wave number in channel region is $K = \sqrt{2m(V_0-E)/\hbar^2}$, therefore the boundary condition implies that the constant parameters can be modeled as:

$$\begin{pmatrix} A_{n+1} \\ B_{n+1} \end{pmatrix} = \begin{pmatrix} e^{-K(b/2)} & e^{K(b/2)} \\ -Ke^{-K(b/2)} & Ke^{K(b/2)} \end{pmatrix} \begin{pmatrix} e^{ik(b/2)} & e^{-ik(b/2)} \\ ike^{ik(b/2)} & -ike^{-ik(b/2)} \end{pmatrix}^{-1} \times \begin{pmatrix} e^{ik(-b/2)} & e^{-ik(-b/2)} \\ ike^{ik(-b/2)} & -ike^{-ik(-b/2)} \end{pmatrix} \times \begin{pmatrix} e^{-K(b/2)} & e^{K(b/2)} \\ -Ke^{-K(b/2)} & Ke^{K(b/2)} \end{pmatrix}^{-1} \begin{pmatrix} A_n \\ B_n \end{pmatrix} \tag{4}$$

The transmission coefficient as a main transport indicator in electrical engineering need to be investigated, while wave propagation in an intermediate part as a transistor channel is interrupted by junction barrier. The transmission coefficient has been explained by transmission amplitude, concentration and total power of a transmitted wave as:

$$t = \frac{-4kKe^{-ikb}}{4kK\cosh(bK) + 2i(k^2-K^2)\sinh(bK)} \tag{5}$$

The transmission coefficient is a scale of how an electromagnetic wave (light) propagates throughout a material[20] which is the transmission amplitude to power of two therefore the transmission coefficient T can be calculated as:

$$T = |t|^2 = \frac{4(K^2/k^2)}{-1+2(K^2/k^2)-K^4/k^4+(1+2(K^2/k^2)+K^4/k^4)\cosh^2(bK)} \tag{6}$$

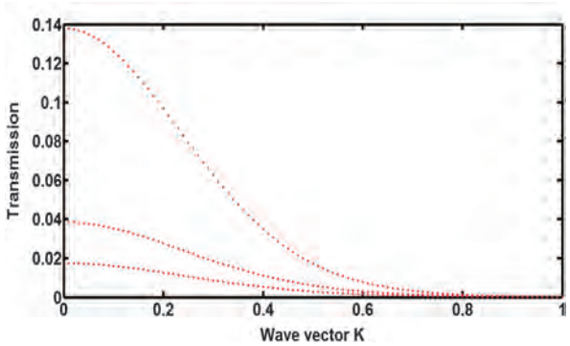

Fig. 3. Transmission for different K values in the GNR at channel region.

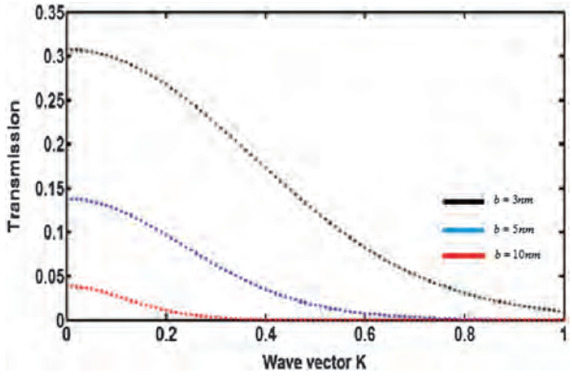

Fig. 5. The transmission variation based on the channel region length (black line indicates channel length 3, blue line for channel length 5 nm and red line shows channel length equal to 10 nm).

Where b is the length of the barrier, the wave vector k outside the barrier is a real quantity for all positive energies E of the electron. The conduction band minimum in the region outside the barrier is taken as the zero of energy. Since the conduction band minimum of the barrier is above that of the region outside hence for certain energies of the electron ($E < V_0$) the wave vector K will be imaginary and for energies above V_0 ($E > V_0$) it will be real. Thus the energy is divided into two regions, ($E < V_0$) for non-classical transition by tunneling and ($E > V_0$) where transition can take place even under classical conditions. Since k and K are both dependent on effective mass and energy, hence for different material pairs the variation of the transmission coefficient for energy values with respect to the barrier height will be different.[26–28] For energies with transmission value equal to 1 the barrier becomes transparent which is called Ramseur Towns effect. When the electron energy E is less than the barrier height V_0 the situation is somewhat different.[29, 30]

The transmission coefficient of electrons through a potential barrier is important for studying the leakage current in MOSFETs with dimensions in the nanometer range. It is also a crucial parameter for studying the behavior of multiple quantum well structures where the barrier is sandwiched between two coupled quantum wells. When both the well and barrier regions are in the nanometer range we expect further quantization of the energy levels. As the barrier width decreases the tunneling increases and transmission coefficient value rises with electron energy. For $E < V_0$, the transmission coefficient increases from 0 to 1 in a non-linear fashion by increasing the wave number as shown in Figures 3, 4 for different regions.

As shown in Figures 3 and 4 if the energy of electron in each region is changed within allowed values the transmission coefficient is varied accordingly. Additionally beyond the normalized energy ($E_n = E/V_0$) > 1, the resonance in the transmission coefficient is observed as shown in Figure 7.

On the other hand, as show in Figures 5 and 6 the manipulation of channel region will affect the transmission property sharply consequently for each pair, the transmission coefficient is lower for wider wells as expected.

It is discovered that the performance of the transmission $T(E)$ is increased rapidly while the energy of the electron is less than the barrier height energy ($E < V_0$) on the other hand for the energies more than the potential barrier the transmission is saturated at 1 as expected. But the presented model needs to be modified for this region to

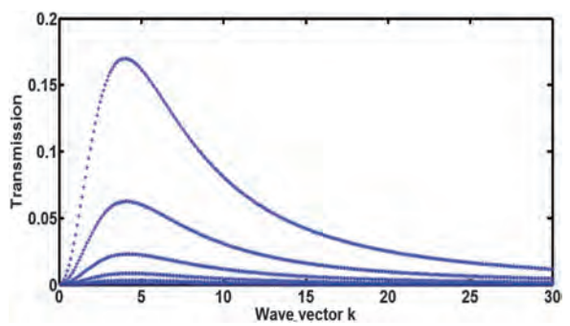

Fig. 4. Transmission for different k values in the GNR at first and third regions.

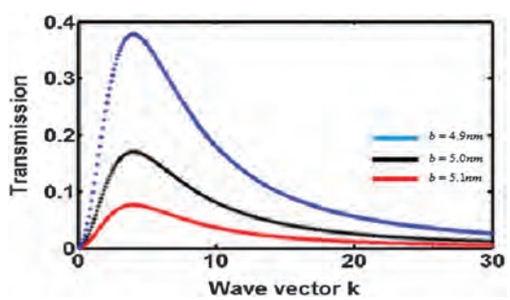

Fig. 6. The transmission variation based on the channel region length (black line indicates channel length 5 nm, blue line for channel length 4.9 nm and red line shows channel length equal to 5.1 nm).

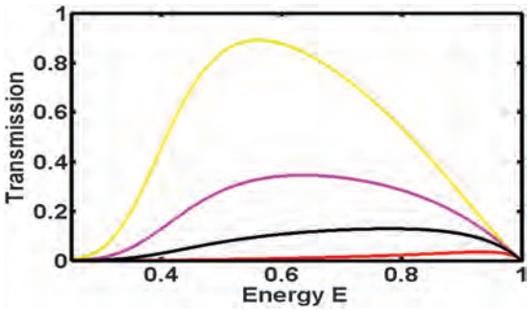

Fig. 7. The transmission variation for energies less than barrier high.

get the accurate results. In the presence of k^2 and K^2 the transmission can be modified as:

$$T(E) = \left(4\frac{V_0 - E}{E}\right) \Big/ \left(-1 + 2\frac{V_0 - E}{E} - \left(\frac{V_0 - E}{E}\right)^2 + \left(1 + 2\frac{V_0 - E}{E} + \left(\frac{V_0 - E}{E}\right)^2\right) \times \cosh^2(\alpha b\sqrt{V_0 - E})\right) \quad (7)$$

Based on the presented model the transmission is analyzed and the numerical result indicates that channel length affects transmission characteristics very fast. As shown in Figure 7 the transmission coefficient for a barrier of height $V_0 = -1$ ev and width 1 nm up to 5 nm varies by channel length. It is notable that for each channel region the optimum electron energy is different and the maximum transmission occurs at 0.45 eV, 0.6 eV, 0.75 eV and 0.9 eV for channel lengths 1 nm, 2 nm, 3 nm and 5 nm respectively. The analyze of the numerical result indicates that by increasing the channel region optimum energy is closer to the barrier height.

It is observed that for all cases the saturation part occurs at $E < V_0$ as shown in Figure 8 therefore for energies more than this value the transmission need to be considered as one.

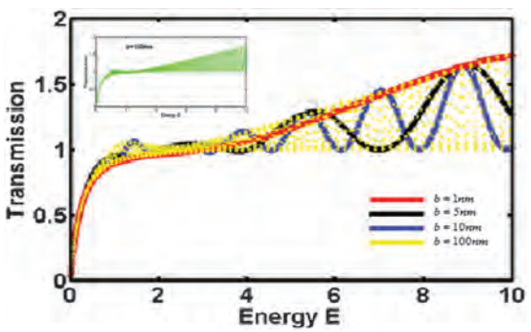

Fig. 8. The T–E characteristic with channel length variation for energies more than barrier height.

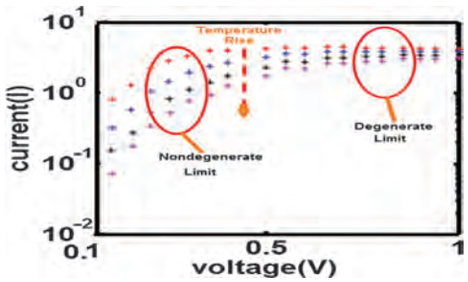

Fig. 9. Current–voltage characteristic of GNR transistor based on the presented model.

As a result, the quantum current based on the Landauer formalism is developed as:

$$I_q = \int_0^{\eta} T(E)F(E)\,dE \quad (8)$$

Where $F(E)$ is Fermi Dirac distribution functions which demonstrate the probability of occupied levels at energy E and leads the current calculation in the form of:

$$I_q = \int_0^{\eta} \left(\left(4\left(\frac{\beta}{T} - 1\right)\right) \Big/ \left(-1 + 2\left(\frac{\beta}{T} - 1\right) - \left(\frac{\beta}{T} - 1\right)^2 + \left(1 + 2\left(\frac{\beta}{T} - 1\right) + \left(\frac{\beta}{T} - 1\right)^2\right) \times \cosh^2\left(\alpha b\sqrt{\frac{V_0}{\beta}(\beta - T)}\right)\right)\right) \frac{1}{1 + e^{x-\eta}}\,dx \quad (9)$$

We define $(E - E_g)/(k_B T) = x$, $(E_g - E_f)/(k_B T) = -\eta$, $\alpha = \sqrt{2m/\hbar^2}$, $\beta = 2V_0/(3K_B)$, K_B is Boltzmann's constant and T is temperature. The temperature dependency on the quantum current is shown in Figure 9 where by increasing the temperature the non-degenerate current is decreased but as usual in the degenerate limit current is going to be saturated in the same amount therefore the effect of temperature in this limit can be neglected.

As shown in Figure 9 the Ohmic response on Current–Voltage (I–V) characteristic for small value of applied bias is observed and the saturation current for the higher voltages are reported. Also from the trend of I–V characteristic it can be concluded that the presented model is works properly.

3. CONCLUSION

Graphene nanoribbon derived from the two-dimensional Graphene has a great impact on the nanoscale transistor performance. Its application on nanoscale device fabrication is expected to run the nanotechnology engine. Among the issues highlighted for GNR is the GNR based device quantum current which contributes to the faster transistor operation and thus expected to alter the carrier mobility. On the other hand, the main parameter that plays important role on device current characteristic is transmission

coefficient. In this paper quantum current of Monolayer Graphene Nanoribbon (MGNR) based on transmission calculation is modeled and the electronic property due to the dependence on structural parameter such as channel length is analyzed.

References and Notes

1. P. Ruffieux, et al., *Nature* 531, 489 **(2016)**.
2. J. Stajic, *Science* 351, 351 **(2016)**.
3. W. Yang, et al., *J. Am. Chem. Soc.* 138, 9137 **(2016)**.
4. P. L. McEwen, et al., *IEEE Transactions on Nanotechnology* 1, 78 **(2002)**.
5. J. A. Misewich, et al., *Science* 300, 783 **(2003)**.
6. J. Chen, et al., *Science* 310, 1171 **(2005)**.
7. A. Javey, et al., *Nature* 424, 654 **(2003)**.
8. J. Li, et al., *Appl. Phys. Lett.* 82, 2491 **(2003)**.
9. J. E. Jang, et al., *Appl. Phys. Lett.* 87, 163114 **(2005)**.
10. J. Kong, et al., *Science* 287, 622 **(2000)**.
11. A. K. Geim and K. S. Novoselov, *Nat. Mater.* 6, 183 **(2007)**.
12. T. O. Wehling, et al., *Science Nano Lett.* 8, 173 **(2004)**.
13. A. H. C. Neto, et al., *Rev. Mod. Phys.* 81, 109 **(2009)**.
14. A. V. Rozhkova, et al., *Physics Reports* 503, 77 **(2011)**.
15. H. Li, et al., *IEEE Transactions on Electron Devices* 56, 1799 **(2009)**.
16. M. Lundstrom and J. Guo, Nanoscale transistors: Device physics, modeling and simulation, Birkhäuser-Technology and Engineering, Springer **(2006)**, 217 pages.
17. H. Kumazaki and D. S. Hirashima, *J. Phys. Soc. Jpn.* 78 **(2009)**.
18. Y. Takane, *J. Phys. Soc. Jpn.* 79 **(2010)**.
19. E. Watanabe, et al., *Phys. Rev. B* 80 **(2009)**.
20. H. Cheraghchi and H. Esmailzade, *Nanotechnology* 21 **(2010)**.
21. S. S. Yu, et al., *IEEE Transactions on Nanotechnology* 9, 78 **(2010)**.
22. A. K. G. K. S. Novoselov, S. V. Morozov, D. Jiang, M. I. Katsnelson, I. V. Grigorieva, S. V. Dubonos, and A. A. Firsov, *Nature* 438, 197 **(2005)**.
23. N. Zydziak, et al., *Polymer Chemistry* 4, 1525 **(2013)**.
24. Y.-Y. Zhang, et al., *Physical Status Solidi a-Applications and Materials Science* 207, 2726 **(2010)**.
25. S. N. hedayat, M. T. Ahmadi, et al., Quantum Current Modelling on Graphene Nanoscrolls, University of Diyala, December **(2015)**, pp. 599–605.
26. B. R. Nag, Physics of Quantum Well Devices, Kluwer Academic Publishers.
27. T. Kuhn and G. Mahler, *Phys. Scr.* 38, 216 **(1988)**.
28. M. D. T. Evans, Quantum Mechanical Tunneling, July **(2012)**.
29. X. Chen and C.-F. Li, *Eur. Phys. J. B* 46, 433 **(2005)**.
30. K. Nakada, M. Fujita, et al., *Physical Review B* 54, 17954 **(1996)**.